

# Optoelectronic and microstructural properties of PANi(EB)-CSA<sub>x</sub> polymer thin films by novel spin coating method

V.B. PATIL<sup>1\*</sup>, S.G. PAWAR<sup>1</sup>, S.L. PATIL<sup>1</sup> and A.K. SOOD<sup>2</sup>

<sup>1</sup>School of Physical Sciences, Solapur University, Solapur - 413 255 (India)

<sup>2</sup>Department of Physics, Indian Institute of Science, Bangalore - 560 002 (India).

(Received: July 10, 2009; Accepted: August 30, 2009)

## ABSTRACT

Films of polyaniline (EB) doped with camphor sulfonic acid (CSA) from *m*-cresol on glass substrates exhibit considerable metallic properties. Such polymer metallic films have thermal sensitivity superior to ceramic metal (Cermet) films, prepared by metallo organic deposition (MOD) technique on silicon substrates. These PANI (EB)-CSA polymer films prepared by oxidation polymerization with doping levels in the range of 10-90%. The electrical conductivity of these films has been measured as a function of temperature between 10 and 300 K. At a doping level of 20% the onset of metallic transport is observed, and at 60% the films are found to exhibit metallic transport down to 135 K, and have a maximum room-temperature conductivity of  $200 \pm 20 \text{ S cm}^{-1}$ . The results are modeled in terms of a heterogeneous model of fluctuation induced tunneling (FIT) and metallic transport. This paper deals with these superior thermal properties together with optical studies and surface morphology by scanning electron microscopy (SEM).

**Key words:** Polyaniline, CSA, SEM, optical properties and electrical properties.

## INTRODUCTION

Conducting polymers have had the attention of researchers for about two decades. A lot of interest is shown due to their relatively large conductivity, light weight and flexibility. These features make them more desirable than metals in certain applications. Much of the past research on conducting polymers has concentrated in the bulk material<sup>1-3</sup>.

Polyaniline (PANI) is continuing to receive considerable interest in the field of conducting polymers. The electrically conductive emeraldine salt form of polyaniline is air stable and cheap to produce in large quantities<sup>4</sup>, giving rise to many suggestions

for possible applications of the material<sup>5</sup>. Until recently the polymer has only been process able in the emeraldine base (EB) form, requiring post-doping with a protonic acid to give the required emeraldine salt (ES). This is not a totally satisfactory processing route as it is difficult to achieve totally homogeneous doping in such dense films<sup>6</sup>. Cao *et al* have recently overcome the problem of processing ES by the discovery of acid solution processing routes<sup>7</sup>. The routes use two specific functional acids, camphor sulfonic acid (CSA) and dodecylbenzene sulfonic acid (DBSA) in organic solvents. One such system has proven to be of considerable interest. This is PANI: CSA in *m*-cresol. Recent work has shown that his material possesses metallic characteristics at high temperatures, i.e. a

positive temperature coefficient of resistivity<sup>8,9</sup>. This behavior has been interpreted in two ways: firstly as indicating that the PANI: CSA is a disordered metal near the metal-insulator boundary<sup>8</sup> and alternatively as being a modified Drude metal-with the modifications being due to localization within the system<sup>9</sup>. It is useful, at this point, to outline what is meant by a disordered metal near the metal-insulator boundary.

This paper reports investigations of the optical properties, microstructural properties and electrically conductive nature of PANI: CSA films with doping level ranging from 10-90%. The conductivity of the samples has been measured as a function of temperature in the range 10-300 K. Definite trends in the temperature dependence of the conductivity have been recorded, with the more highly doped samples showing the previously observed positive temperature coefficient of resistivity indicative of metallic behaviour.

## EXPERIMENTAL

### Preparation of Polyaniline (EB)

50 ml 1M HCl, and 2ml of aniline were added into a 250 ml flask (covered with ice cubes-salt mixtures to maintain low polymerization temperature) equipped with electromagnetic stirrer. Then 4.9984 g of  $(\text{NH}_4)_2\text{S}_2\text{O}_8$  (Ammonium peroxydisulphate) in 50 ml, 1M HCl was suddenly added into the above solution. The polymerization temperature  $+30^\circ\text{C}$ ,  $0^\circ\text{C}$  and  $-30^\circ\text{C}$  were maintained for 5 h to complete the reaction. Then the precipitate obtained was filtered. The product was washed successively by 1M HCl followed by distilled water and respectively until the wash solution turned colorless. Then it was re-filtered and washed once again successively by distilled water, thoroughly to obtain the emeraldine salt form of polyaniline. To obtain emeraldine base form of PANI, dedope ES from of PANi with 0.1M  $\text{NH}_4\text{OH}$  solution then dried at  $60^\circ\text{C}$  in vacuum for 24 h. Thus, finally obtained powder of insulating polyaniline (EB) polymer and its structure is shown in figure 1.

### Preparation of camphor sulfonic acid (CSA) doped PANI

PANI (EB) was synthesized by solid state reaction using the procedure reported by Reghu *et*

*al*<sup>10</sup>. PANI-CSA was prepared by mixing 1.092 gm (0.012 M) of emeraldine base with 1.394 gm (0.006 M) of ( $\pm$ ) 10 camphor sulfonic acid using agate mortar and pestle. The molar ratio of PANI: CSA was 1:0.5. PANI-CSA is soluble in various organic solvents<sup>11</sup>; for this study, high quality films were prepared by casting the material from solution metacresol<sup>12</sup>. The films were prepared from 4% (by weight) solution of PANI-CSA in metacresol. The solutions were prepared by adding an appropriate quantity of PANI – CSA into metacresol (1.0 gm of PANI-CSA to 24 ml of *m*-cresol to yield a 3.9% solution) the mixture was then treated in an ultrasonic bath for 12 hrs and subsequently centrifuged. Most of the PANI-CSA complex dissolved to give a deep green solution; minor insoluble solids were removed by decanting. PANI-CSA films were thus obtained by casting films on glass plates using spin coater and subsequently dried for 24 hrs on a hot plate at  $50^\circ\text{C}$ . Film thicknesses were determined by ellipsometry and it was typically from 8-20  $\mu\text{m}$ . Since the PANI-CSA films cast from solution, the PANI chains are neither chain extended nor chain aligned. The films are therefore in all respect isotropic.

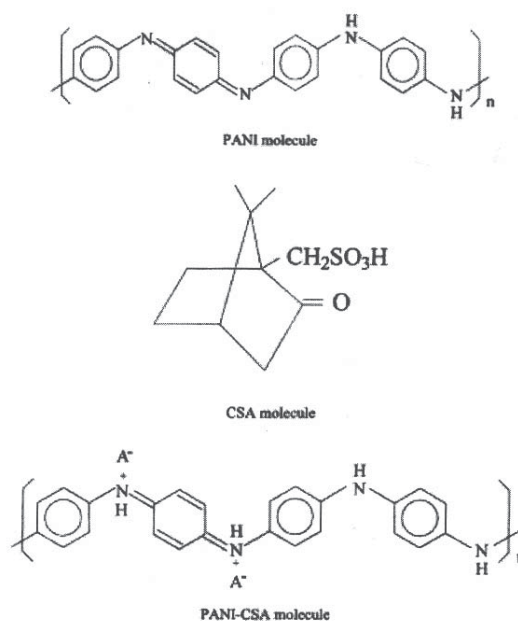


Fig. 1: The molecular structure of PANI-CSA molecule

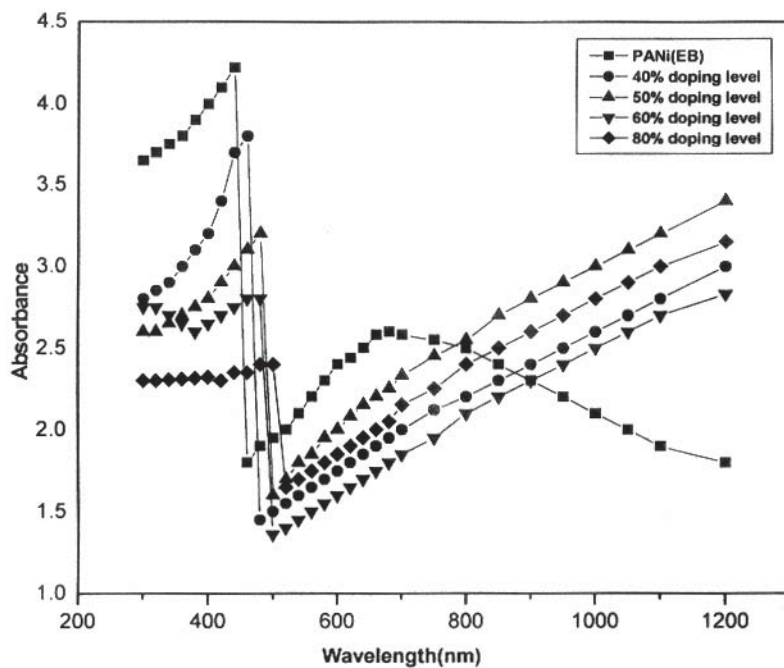


Fig. 2: Absorption spectra of PANI (EB)-CSAx polymer thin film

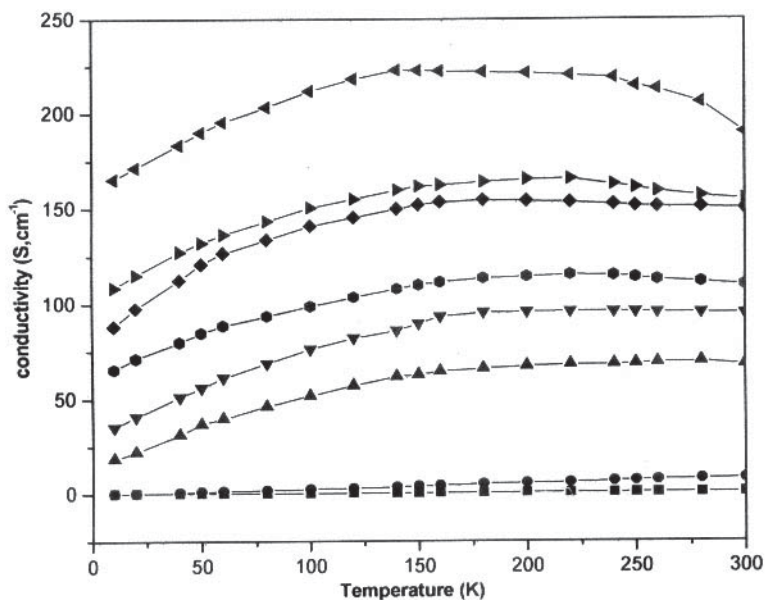


Fig. 3: Conductivity of PANI (EB)-CSAx as a function of temperature for films of various doping level

a) ■ = 10%, b) ○ = 20%, c) △ = 30%, d) ▽ = 40%, e) ◆ = 50%, f) ▲ = 60%, g) ● = 70% and h) ○ = 80%.

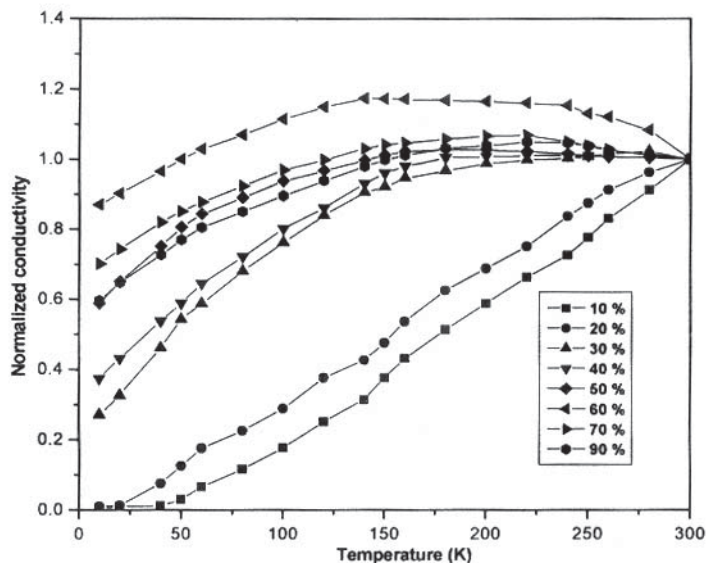


Fig. 4: Normalized conductivity of PANI (EB)-CSAx ( $\sigma(t)/\sigma(300K)$ ) as a function of temperature for films of various doping levels (10-90%)

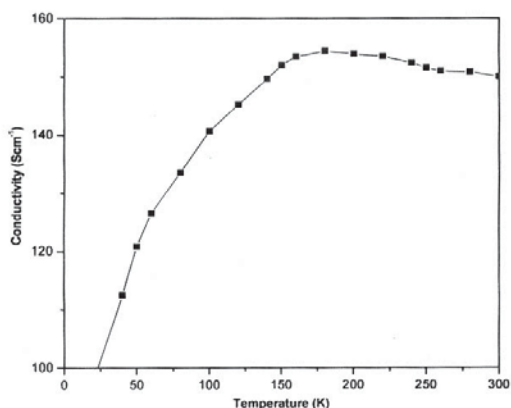


Fig. 5: A linear plot of conductivity of PANI (EB)-CSA as a function of temperature for a 50% doped film

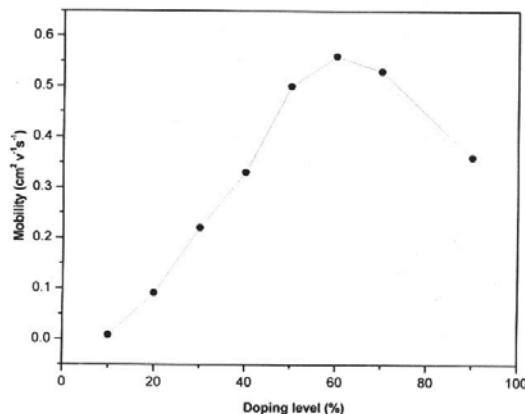


Fig. 6: A plot of the charge carrier mobility of PANI (EB)-CSAx (at room temperature) as a function of doping level

The optical absorption spectra were recorded at room temperature by 'Hitachi 330 Model Spectrophotometer' in the wavelength region 200-1200 nm for both PANI (EB) and PANI (EB)-CSAx ( $X = 40\%$ ,  $50\%$ ,  $60\%$  and  $80\%$  doping level) polymer films. The electrical conductivity of PANI-CSA at room temperature was measured by four probe technique using Keithley 2000 Multimeter. The surface morphologies of the PANI (EB) and PANI-CSA were observed by scanning electron microscope (SEM) using a Quanta-200, Holland.

## RESULTS AND DISCUSSION

### Optical Characteristics

Optical absorption spectra of PANI (EB) and PANI (EB)-CSA polymer films for different doping levels were recorded in the wavelength region 200-1200 nm. Typical absorption spectra for all polymer films are shown in Fig. 2. The uncertainties in the absorbance values are within the  $\pm 0.002$  nm. The UV-visible absorption spectra of PANI (EB) in metacresol solution cast film gives

absorption bands at 440 nm and 690 nm. In this case, the  $\lambda_{\text{max}}$  (wavelength of an absorption maximum) is 440 nm and this band has been assigned as the  $TT - TT^*$  transition and the band at 690 nm is due to electron band arising due to the shifting of electron from benzenoid ring to quinoid ring. In all the doped polyaniline cases, only the  $TT - TT^*$  transition band alone of PANI (EB)-CSA, 40% doping level at 450 nm, PANI (EB)-CSA 50% doping level at 454 nm, PANI (EB)-CSA 60% doping level at 460 nm, PANI (EB)- to the infrared without absorption peak at 690 nm. So, the red shift occurs in all the CSA 80% doping level at 464 nm is given. The doping of PANI (EB) with the CSA converts the insulating nature of PANI (EB) into conducting state (metallic nature) because the protons of CSA are added to  $-N=$  sites while the number of electron in the chain are constant. Because of this reason all the doped polymer films absorption spectra extend to the infrared without absorption peak at 690 nm. So, the red shift occurs in all doped cases.

### Electrical Characteristics

Figure 3 shows the plots of conductivity versus temperature for the films with doping levels between 10 to 90%. It is clear that as the level of protonation is increased from 10 to 60% the conductivity increase rapidly. At 10 K the 60% doped sample is five orders of magnitude more conductive than the 10% doped sample. Also, the conductivity becomes a weaker function of temperature in the more heavily protonated films. The normalized conductivity,  $\sigma(T)/\sigma(300\text{ K})$ , for each data set are shown in figure 4, and allow the trend in conductivity of each sample with temperature to be compared more easily.

At the two lowest levels of protonation (10 and 20%) the conductivity rises monotonically as temperature is increased. Additionally, the rate of increase of  $\sigma(T)$  increases with temperature. When the protonation level reaches 30% and above, the data reveal a very different behaviour. At low temperatures, conductivity increases as temperature rises, but at higher temperatures, this rate of increase decreases. Moreover, each data set in the 30-90% doping range possesses a characteristic maximum in  $\sigma(T)$  somewhere in the measured range. In table 1 typical peak positions and their accompanying conductivity values are presented. For each case, at temperatures above that at which the peak occurs, the conductivity decreases slowly with increasing temperature i.e. the electrical conductivity has a negative temperature coefficient. In figures 5 the data for the 50% doped sample are presented on a linear scale to reveal in detail the temperature dependence of the conductivity of highly conductive PANI: CSA.

It is widely accepted that the density of charge carriers within samples of conductive polyaniline is approximately equal to the density of protonated chain sites, up to a protonation level of 50%. If it is assumed that all the CSA dopants added to the polymer causes protonation above 50%, and that this increase in protonation causes an increase in charge carriers even where the theoretical 50% level is exceeded, it is possible to estimate the charge carrier density in samples prepared. Furthermore, using the general expression for electrical conductivity.

$$\sigma = ne\mu$$

**Table 1: Temperature values at which the conductivity maxima occur in of PANI (EB)-CSAx**

Protonation (%)	Peak conductivity (S cm <sup>-1</sup> )	Peak temperature (K)	$\sigma(10\text{K})/\sigma(300\text{ K})$
30	69.58	280	0.27
40	96.06	220	0.37
50	154.50	180	0.59
60	222.80	150	0.87
70	165.72	210	0.70
90	115.50	220	0.60

It is possible to make an estimate of the charge carrier mobility,  $\mu$ , where  $n$  is the carrier density and  $e$  is the charge on an electron. The results of these calculations are shown graphically in figure 6. The reduction of mobility at the higher doping levels (90%) may well be due to a breakdown of the previous assumption.

From these results it would appear that there are two distinct regimes of charge transport

in this material according to the level of protonation to which it is prepared. Samples prepared at 10 and 20% protonation, the two lowest doping levels, display an electrical conductivity which is a strong function of temperature, suggestive of charge carriers dependent upon some form of thermal activation. The variable-range hopping mechanism (VRH), in one or two dimensions, has been used to describe the charge transport observed in PANi from previous studies<sup>13-15</sup>. However, none of the data in

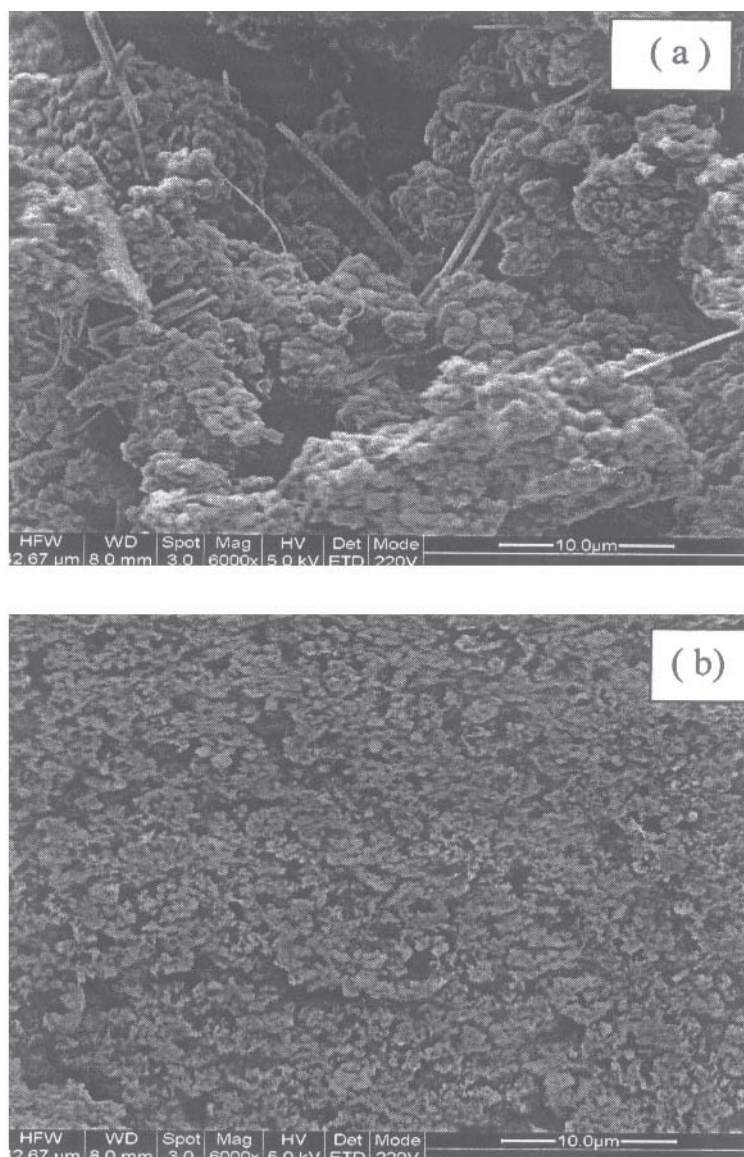


**Fig. 7: Scanning electron microscopy photographs of a) PANi (EB); b) PANi-CSA (for 50% doping level)**

figure 3 are characteristic of transport by VRH. At temperatures above 100 K the 10 and 20% samples can be described by the fluctuation induced tunneling (FIT) model, which has the form

$$\sigma = \sigma_0 \exp [-T_1/T + T_0]$$

where  $T_1$  depends upon the average potential barrier height and  $T_0$  represents the temperature for which the thermal fluctuations produce a significant contribution to the tunneling current compared with the temperature independent elastic tunneling. At lower temperatures, however, the fit to these data based upon the form of this equation deviates significantly from the measured values.

A very different trend is revealed by the samples prepared with protonation levels in the range 30-90%. At low temperatures the conductivity still displays an activated behaviour. As the level of protonation is increased from 30% the decreases in the conductivity at the lowest temperatures is much reduced, as illustrated by the values of  $\sigma(T)/\sigma(300\text{ K})$  in each case.

The results presented here suggest that the metallic behaviour extends to the lowest temperatures with the 60% protonated film, and that this doping level also results in the highest electrical conductivity. From figure 3, it is also evident that the reduction of conductivity at low temperatures is the least pronounced for the 60% doped films. This evidence implies that doping above the 50% level is capable of driving the PANI: CSA system far closer to the true metallic behaviour than observed in previous studies. Two explanations are suggested for why this may occur.

- ' Samples prepared with 50% doping do not react completely with the CSA added to the polymer. An excess of 10 ( $\pm 5$ ) % acids is required to protonate all the imine sites on the polymer chain.
- ' Protonation of more than 50% of the nitrogen sites generated more conduction band state and allows a higher charge carrier density within the material, up to a maximum at 60%.

### Surface Morphology

The morphology, shape and size of PANI (EB) and PANI-CSA particles determined by SEM are shown in figure 7. SEM of PANI (EB) (fig. 7 a) shows closer interspection reveal that the aggregates are all perforated and porous, much like a honeycomb with an interlocking arrangement of globular particles<sup>16,17</sup>. In addition the images of nano tubes observed with diameter in the range of 84 nm to 120 nm<sup>17</sup>. For PANI-CSA, SEM image (fig. 7b), the shape of the particle is very fine and the size range of the particles is approximately 50 nm to 100 nm.

### CONCLUSIONS

The present investigations of PANI-CSA polymer films produced by spin coating method with doping levels in the range 10-90%. The UV-visible absorption spectra of PANI (EB) in *m*-cresol solution cast film gives absorption bands at 440 nm and 690 nm. In this case, the  $\lambda_{\text{max}}$  (wavelength of an absorption maximum) is 440 nm and this band has been assigned as the  $p-p^*$  transition and the band at 690 nm is due to electron band arising due to the shifting of electron from benzenoid ring to quinoid ring. In all the doped polyaniline cases, only the  $p-p^*$  transition band alone of PANI(EB)-CSA, 40% doping level at 450 nm, PANI(EB)-CSA 50% doping level at 454 nm, PANI (EB)-CSA 60% doping level at 460 nm, PANI (EB)-CSA 80% doping level at 464 nm is given.

The conductivity of the PANI: CSA films have been measured as a function of temperature in the range 10-300 K with doping levels in the range 10-90%. It has been shown that there are two distinct regimes of conductive behaviour. Below 30% doping the films have very low conductivity that fits a fluctuation induced tunneling model above 100 K. At doping levels of 30% and above the films start to show metallic behaviour above some doping dependent critical temperature. The data for these films fit a heterogeneous model of conductivity; combining fluctuation induced tunneling with metallic conductivity. Calculation of the mobility of the charge carriers in the films of various doping levels reflects the transition between the two forms of conductive behaviour. The films with a doping level of 60% have

been found to exhibit the highest room-temperature conductivity, and metallic behaviour down to the lowest temperatures.

Scanning electron microscopy of PANI (EB) reveals honeycomb structure with an interlocking arrangement of gobular particles, in addition the images of nano tubes observed with diameter in the range of 84 nm to 120 nm, while for PANI: CAS SEM image, the shape of the particle is very fine and size range of the particles is

approximately 50 nm to 100 nm.

#### ACKNOWLEDGMENTS

One of the authors (VBP) is thankful to Jawaharlal Nehru Centre for Advanced Scientific Research, Bangalore for awarding Visiting Fellowship (2007). Thanks are due to all Group members of Prof. A. K. Sood Laboratory, Department of Physics, Indian Institute of Science, Bangalore, providing the necessary support.

#### REFERENCES

- MacDiarmid, A. G., Jones, W. E., Norris, I. D., Gao, J., Johnson, A. T., Pinto Jr, N. J., Home, J., Han, B., Ko, F., Okuzaki, K. H. and Llaguno, M., *Synth. Met.*, **119**: 27-30 (2001).
- Huang J., Virji S., Weiller B. H. and Kaner, R. B., *J. Am. Chem. Soc.*, **125**: 314-315 (2003).
- Adams, P. N., Devasagayam, P., Pomfret, S. J. Abell, L. and Monkman, A. P., *J. Phys.: Condens. Matter*, **10**: 82-93 (1998).
- Salaneck, W. R., Clark, D. T. and Samuelsen, E. J., (ed) *Science and Applications of Conducting Polymers* (Bristol: Hilger) (1991).
- Epstein, A. J. and MacDiarmid, A. G., *Synth. Met.*, **69**: 179 (1995).
- Monkman, A. P. and Adams, P. N., *Synth. Met.*, **627**:41-43 (1991).
- Cao, Y., Smith, P. and Heeger, A. J., *Synth. Met.* **48**: 91 (1992).
- Menon, R., Yoon, C.O., Moses, D. and Heeger, A. J., *Phys. Rev.*, **B 48**: 685 (1993).
- J Jao, E. J. Oh, G. Min, A. G. MacDiarmid and A. J. Epstein, *Synth. Met.*, **69**: 251 (1995).
- Reghu, M. and Heeger A. J., *Physical Review*, **B 47(4)**: 1758 (1993).
- Cao, Y., Smith, P. and Heeger A. J., *Synthetic metals*, **48**: 91 (1992).
- Cao, Y., Smith, P. and Heeger, A. J., *Appl. Phys. Lett.*, **60**: 1 (1992).
- Jeong, S. K., Suh, J. S., Oh, E. J., Park, Y. W., Kim, C. Y. and MacDiarmid, A. G., *Synth. Met.*, **69**: 171 (1995).
- Park, Y. W., Lee, Y. S., Park, C., Shacklette, L. W. and Boughman, R. H., *Solid State Commun.*, **63**: 1063 (1987).
- Zuo, F., Angelopoulos, M., MacDiarmid, A. G. and Epstein, A. J., *Phys. Rev.*, **B 36**: 3475 (1987).
- Goel, S., Gupta, A., Singh, K. P., Mehrotra, R. and Kandpal, H. C., *Materials Science and Engineering*, **A 443**: 71 (2007).
- Wei Pan, Sheng Lin Gang Guang Li, and Jian Ming Jiang, *European Polymer Journal*, **41**: 2127 (2005).